GEOPHYSICAL RESEARCH LETTERS, VOL. 35, L19107, doi:10.1029/2008GL034869, 2008



# Properties of the termination shock observed by Voyager 2

H. Li,[1,2] C. Wang,[1] and J. D. Richardson[3]

Received 2 June 2008; revised 24 August 2008; accepted 2 September 2008; published 9 October 2008.

[1] In August 2007, Voyager 2 reached the termination shock and entered the heliosheath at a distance of about 83.6 AU. Due to the variations of the solar wind dynamic pressure or waves on the shock front, the termination shock moved back and forth, and Voyager 2 crossed the termination shock multiple times. We use the best fit solution of the Monte-Carlo method to define the upstream and downstream conditions and determine the properties of termination shock, such as the shock normal, speed, and strength. For the crossings on DOY 243.819-243.875(shock 1) and DOY 243.99-244.012(shock 2), the termination shock moved almost in the radial direction. The shock is nearly perpendicular, and the angle between the shock normal and the solar wind magnetic field is about 70°. In the case of the first crossing, the termination shock moved away from the Sun with a speed of about 100 km $s^{-1}$, whereas the termination shock moved toward Sun with a speed of about 30 km $s^{-1}$ for the second crossing. The density ratios of the termination shock are 2.2 and 1.6, respectively. For both crossing events, the flow is found to be still supersonic with respect to the thermal ions downstream of the termination shock, probably due to the fact that most of the solar wind energy is transferred to the pickup ions. **Citation:** Li, H., C. Wang, and J. D. Richardson (2008), Properties of the termination shock observed by Voyager 2, *Geophys. Res. Lett.*, *35*, L19107, doi:10.1029/2008GL034869.

## 1. Introduction

[2] The interaction of the solar wind with the local interstellar medium results in the formation of heliospheric boundaries, including the termination shock, the heliopause, and perhaps a helio-bowshock. Generally speaking, the termination shock marks the transition where the solar wind slows from supersonic to subsonic speed, and where there are large changes in the orientation of the Sun's magnetic field and the direction of flow of charged particles. This shock is expected to be a fast mode reverse MHD shock. The location of the termination shock had been estimated to be ~80–120 astronomical units (AU) [*Zank*, 1999], depending on the solar wind and the local interstellar medium conditions. Even though Voyager 1 made the first crossing of the termination shock in December 2004, the properties of the termination shock were not fully understood since (1) the shock crossing occurred in a data gap and (2) there was no working plasma instrument that could directly measure the velocity, density and temperature of the solar wind.

[3] On August 30, 2007, Voyager 2 reached the termination shock region and entered the heliosheath at a distance of about 83.6 AU [*Stone et al.*, 2008; *Richardson et al.*, 2008; *Burlaga et al.*, 2008]. Due to the variations of the solar wind dynamic pressure and/or waves on the shock front, the termination shock moved back and forth [*Wang and Belcher*, 1999], which caused multiple crossings of the termination shock by Voyager 2. Voyager 2 had at least five shock crossings spaced over a couple of days. We pick up two shock crossings in the interval between 20:00 August 31 – 00:00 September 1, 2007, which have the best data coverage and derive shock properties, such as the shock normal, speed, and strength. This information is of great importance for understanding the characteristics of the termination shock, its formation, and movement.

## 2. Shock Parameters

[4] To study MHD shocks, it is important to identify the shock frame of reference and shock parameters accurately. All of the shock parameters have to satisfy the Rankine-Hugoniot relations [e.g, *Chao*, 1970]. In searching for an accurate shock frame of reference, determining the shock normal from the observations is the first step. Many methods have been proposed to find the accurate shock normal vector in the literature. For example, using the upstream and downstream velocities ($\vec{V}_1$, $\vec{V}_2$) only, *Abraham-Shrauner* [1972] has determined the shock normal vector as:

$$\hat{n} \simeq \pm(\vec{V}_2 - \vec{V}_1)/|\vec{V}_2 - \vec{V}_1| \quad (1)$$

[5] However, this approximation is valid only for a very high Alfven Mach number shock (for a very large upstream flow velocity and/or a very small upstream magnetic field intensity). *Colburn and Sonett* [1966] proposed the magnetic coplanarity theorem for isotropic plasmas, which demonstrates that the magnetic fields on both sides of a shock and the shock normal vector lie in the same plane. The situation in anisotropic plasmas has also been generalized by *Chao* [1970]. Under this framework, only observed magnetic fields data (upstream: $\vec{B}_1$, downstream: $\vec{B}_2$) are needed to calculate the shock normal vector (Equation 2).

$$\hat{n} = \pm \frac{(\vec{B}_2 - \vec{B}_1) \times (\vec{B}_2 \times \vec{B}_1)}{|(\vec{B}_2 - \vec{B}_1) \times (\vec{B}_2 \times \vec{B}_1)|} \quad (2)$$

*Abraham-Shrauner* [1972] suggested a mixed data method, namely velocity-magnetic field coplanarity, which requires

[1]State Key Laboratory of Space Weather, Center for Space Science and Applied Research, Chinese Academy of Sciences, Beijing, China.
[2]Graduate School of Chinese Academy of Sciences, Beijing, China.
[3]Kavli Institute for Astrophysics and Space Research, Massachusetts Institute of Technology, Cambridge, Massachusetts, USA.


0094-8276/08/2008GL034869$05.00

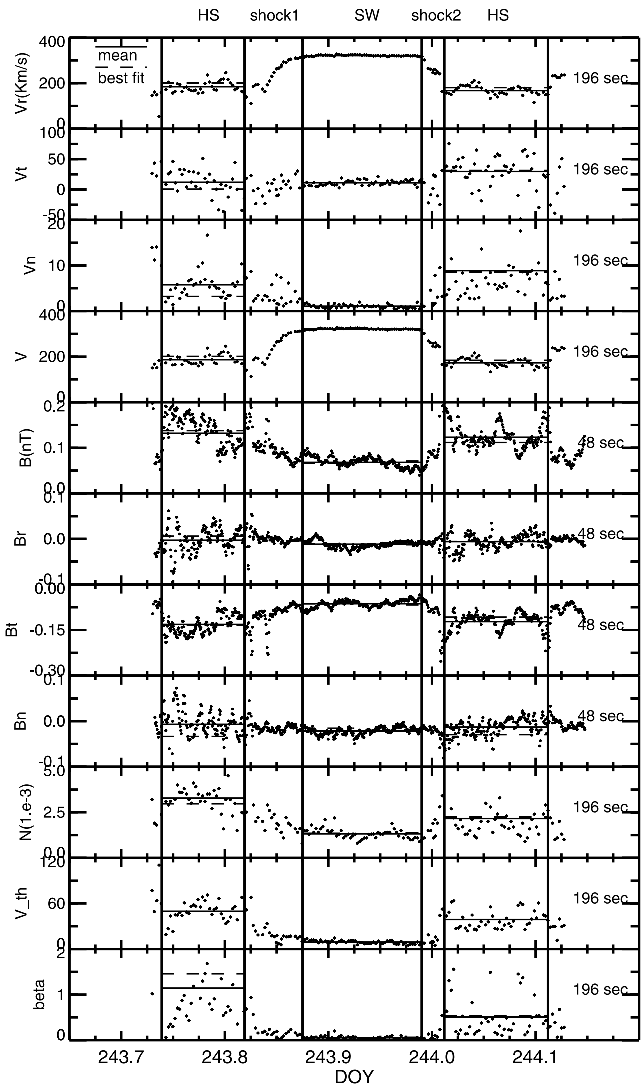


**Figure 1.** Observations of the termination shock crossing events by Voyager-2 from Aug. 31, to Sept. 1, 2007.

both the velocity and magnetic field data on both sides of the shock to obtain the shock normal vector (Equation 3).

$$\hat{n} = \pm \frac{\vec{B}_1 \times \left(\vec{V}_2 - \vec{V}_1\right) \times \left(\vec{B}_2 - \vec{B}_1\right)}{\left|\vec{B}_1 \times \left(\vec{V}_2 - \vec{V}_1\right) \times \left(\vec{B}_2 - \vec{B}_1\right)\right|} \tag{3}$$

[6] The plasma velocity and magnetic field data from 17:25 August 31 (DOY, Day of Year = 243), 2007 to 03:02 September 1 (DOY = 244), 2007 are plotted in Figure 1, which shows clearly the multiple crossing events. Figure 1 shows, from top to bottom, the plasma velocity vector components ($V_r$, $V_t$, $V_n$), speed ($V$), magnetic field strength (B), magnetic field vector components ($B_r$, $B_t$, $B_n$), the proton number density ($N$), the proton thermal speed ($V_{th}$), and the ion plasma beta ($\beta$), respectively. The vector components are all given in the RTN coordinate system, where r is radially outward, t is in a plane parallel to the solar equatorial plane and positive in the direction of solar rotation, and n completes a right-handed system. The time resolution of the data are also indicated in Figure 1.

[7] Two obvious jumps in the plasma parameters occur in the time intervals of DOY 243.819-243.875 and DOY 243.99-244.012, which correspond to the two shock crossing events, which are labeled shock 1 and shock 2 in Figure 1. The time interval DOY 243.875-243.99 has high speed, low magnetic field and density, which is, of course, in the solar wind region. The time intervals DOY 243.739-243.819 and 244.012-244.112 have low speed, high magnetic field and density, which are in the heliosheath.

[8] To study the properties of the termination shock, we should first accurately determine the shock normal vector. To make comparisons, we use all three methods mentioned above to calculate the shock normal. The method using equation (1) is called Mth 1, and the same for Mth 2 and 3 which use equations (2) and (3), respectively. In order to obtain the upstream and downstream parameters more accurately, we use the Monte-Carlo method, which was first introduced to shock fitting procedures by *Lin et al.* [2006].

[9] Based on the observed means and standard deviations, the Monte-Carlo method is used to generate arrays for the 15 variables as follows:

$$\widetilde{X}\left(\widetilde{\vec{B}}_{1,2}, \widetilde{\vec{W}}, \widetilde{\rho}_{1,2}, \widetilde{\beta}_{1,2}, \widetilde{\xi}_{1,2}\right) = X_{mean} + Rnd(SD) \tag{4}$$

where ($\vec{B}_1$, $\vec{B}_2$) are the upstream and downstream magnetic fields, ($\rho_1$, $\rho_2$) are the plasma mass densities, ($\xi_1$, $\xi_2$) are the plasma anisotropies, ($\beta_1$, $\beta_2$) are the plasma betas, and ($\vec{W}$) is the difference between the downstream and upstream velocities. We use a random number generator function, called Rnd(SD) and the mean of the sample $X_{mean}$ to generate the $\widetilde{X}$(i) array, where i = 1,2..,N. SD is the sample standard deviation. A loss function is introduced to measure how well the variables can fit the observed means:

$$L(i) = \sum_{k=1,15} \left[\frac{X_k(i) - \langle X_k \rangle}{\sigma_k}\right]^2 \tag{5}$$

$\langle X_k \rangle$ represents the mean of each observable $X_k$. The $\sigma_k$ is defined as the sum of the SD and the systematic errors. The best estimate of the variables is defined to be the value that minimizes the loss function. Unlike *Lin et al.* [2006], we choose $X_k \equiv (\vec{B}_1, \vec{B}_2, \rho_1, \rho_2, \vec{W}, \beta_1, \beta_2)$ independently to get the best estimate of ($\vec{B}_1$, $\vec{B}_2$, $\rho_1$, $\rho_2$, $\vec{W}$, $\beta_1$, $\beta_2$) instead of $X_k \equiv (\vec{B}_1, \vec{B}_2, \rho_1, \rho_2, \vec{W}, \beta_1, \beta_2, \xi_1, \xi_2)$ because of the absence of the data of anisotropy parameters($\xi_1$, $\xi_2$).

**Table 1.** Means and Standard Deviations of the Upstream and Downstream Conditions of Shock 1

| Observation | Mean | Standard Deviation |
|---|---|---|
| $\vec{B}_1(nT)$ | (−0.012,−0.063,−0.022) | (0.008,0.012,0.008) |
| $\vec{B}_2(nT)$ | (−0.003,−0.132,−0.007) | (0.028,0.030,0.033) |
| $N_1$(cc) | 0.0013 | 0.0003 |
| $N_2$(cc) | 0.0033 | 0.0009 |
| $\beta_1$ | 0.053 | 0.032 |
| $\beta_2$ | 1.143 | 0.897 |
| $\vec{V}_1$(km/s) | (321.01,11.26,1.07) | (2.84,4.29,0.45) |
| $\vec{V}_2$(km/s) | (184.67,11.89,5.77) | (23.38,22.40,2.95) |

**Table 2.** Means and Standard Deviations of the Upstream and Downstream Conditions of Shock 2

| Observation | Mean | Standard Deviation |
|---|---|---|
| $\vec{B}_1(nT)$ | (−0.012,−0.063,−0.022) | (0.008,0.012,0.008) |
| $\vec{B}_2(nT)$ | (−0.006,−0.122,−0.013) | (0.017,0.027,0.018) |
| $N_1$(cc) | 0.0013 | 0.0003 |
| $N_2$(cc) | 0.0022 | 0.0012 |
| $\beta_1$ | 0.053 | 0.032 |
| $\beta_2$ | 0.508 | 0.428 |
| $\vec{V}_1$(km s) | (321.01,11.26,1.07) | (2.84,4.28,0.45) |
| $\vec{V}_2$(km s) | (167.63,29.68,8.87) | (19.72,26.33,9.63) |

[10] The means and standard deviations of the upstream and downstream conditions of shocks 1 and 2 are given in Tables 1 and 2, respectively. The best fit solutions for shock 1 and shock 2 from the Monte-Carlo calculation method are given in Table 3, where we use $\xi_1 = 1.0$, $\xi_2 = 1.0$ for both shock structures.

[11] We calculate the shock normal vector $\hat{n}$ with the three methods mentioned above, and other shock parameters, such as density ratio ($y = N_2/N_1$), magnetic field intensity ratio ($m = B_2/B_1$), tangential magnetic field ratio ($u = B_{t2}/B_{t1}$), tangential velocity ratio ($z = V_{t2}/V_{t1}$), the angle between the shock normal vector and upstream magnetic field vector ($\theta_{BN}$), the angle between the shock normal vector and downstream magnetic field vector ($\theta_{BN2}$), the upstream Alfven speed ($V_A$), the downstream Alfven speed ($V_{A2}$), the upstream Alfven Mach number ($M_A$), the downstream Alfven Mach number ($M_{A2}$), the upstream normal Alfven Mach number ($M_{AN}$), the downstream normal Alfven Mach number ($M_{AN2}$), the upstream fast Mach number ($M_F$), the downstream fast Mach number ($M_{F2}$), and two additional parameters (the equivalent "normal momentum" and "energy" additions $\Delta G$ and $\Delta Q$) introduced in the modified Rankine-Hugoniot relation model (see *Lin et al.* [2006] for details). The results using means direct from the observation are given in Table 4, while the results using the best fit solution of the Monte-Carlo method are given in Table 5.

[12] Table 4 shows that the shock normal calculated from Mth 1 is significantly different from the other two methods. This difference might imply that the means of the upstream and downstream conditions chosen do not reflect the real situations, either due to observational errors or to incorrectly chosen time intervals. However, when we use the best fit solutions of the Monte-Carlo method to calculate the shock normal vector as given in Table 5, the differences between these three method are negligible. The means of the observations and the best fit solutions from the Monte-Carlo method are plotted in Figure 1 as solid and dashed lines, respectively. Thus, we believe that the best fit solutions from the Monte-Carlo method give more accurate upstream and downstream conditions of the termination shock. Nevertheless, these results are roughly in agreement with those estimations obtained without using the Monte-Carlo approach [*Richardson et al.*, 2008]. An interesting result is that the flow is still supersonic with respect to the thermal plasma downstream of the termination shock, probably due to the fact that most of the solar wind flow energy is transferred to the pickup ions instead of going into heating the thermal plasma [*Richardson et al.*, 2008]. For the crossing event during DOY 243.819-243.875 (shock 1), the termination shock moves mainly in the radial direction with a speed of about 100 km s$^{-1}$, which means that the termination shock moves away from the Sun and crosses

**Table 3.** Best Fitting Results by Using Monte-Carlo Method

| Observation | Shock 1 | Shock 2 |
|---|---|---|
| $\vec{B}_1(nT)$ | (−0.011,−0.063,−0.016) | (−0.013,−0.067,−0.018) |
| $\vec{B}_2(nT)$ | (0.006,−0.133,−0.034) | (−0.006,−0.107,−0.030) |
| $N_1$(cc) | 0.0014 | 0.0014 |
| $N_2$(cc) | 0.0030 | 0.0022 |
| $\beta_1$ | 0.045 | 0.063 |
| $\beta_2$ | 1.457 | 0.534 |
| $\vec{V}_1$(km/s) | (321.01,11.26,1.07) | (321.01,11.26,1.07) |
| $\vec{V}_2$(km/s) | (200.98,0.66,3.20) | (180.71,31.40,8.58) |

**Table 4.** Calculated Results of Shock Properties Using the Observed Means

| | Shock 1 | | | Shock 2 | | |
|---|---|---|---|---|---|---|
| | Mth1 | Mth2 | Mth3 | Mth1 | Mth2 | Mth3 |
| $\hat{n}$ | 0.999 | 0.477 | 0.991 | 0.992 | 0.495 | 0.995 |
| | −0.005 | 0.243 | 0.131 | −0.119 | 0.173 | 0.101 |
| | −0.034 | 0.845 | 0.013 | −0.050 | 0.852 | 0.025 |
| y | 2.5 | 2.5 | 2.5 | 1.6 | 1.6 | 1.6 |
| m | 1.9 | 1.9 | 1.9 | 1.8 | 1.8 | 1.8 |
| u | 2.0 | 2.3 | 2.0 | 1.8 | 2.0 | 1.9 |
| z | 0.8 | 0.9 | 0.8 | 1.1 | 1.2 | 1.1 |
| $\theta_{BN}$ | 80.9 | 54.8 | 72.7 | 87.5 | 58.9 | 74.1 |
| $\theta_{BN2}$ | 85.3 | 72.7 | 81.2 | 88.6 | 73.4 | 81.3 |
| $V_A$ | 40.8 | 40.8 | 40.8 | 40.8 | 40.8 | 40.8 |
| $V_{A2}$ | 50.2 | 50.2 | 50.2 | 57.7 | 57.7 | 57.7 |
| $V_{sn}$ | 92.6 | 54.9 | 54.9 | −78.6 | −7.2 | −64.4 |
| $M_A$ | 5.6 | 2.5 | 4.5 | 9.7 | 4.1 | 9.4 |
| $M_{A2}$ | 1.8 | 0.8 | 1.8 | 4.2 | 1.8 | 4.1 |
| $M_{AN}$ | 35.5 | 4.3 | 18.6 | X[a] | 8.0 | 34.4 |
| $M_{AN2}$ | 22.5 | 2.7 | 11.8 | X[a] | 6.3 | 26.9 |
| $M_F$ | 5.5 | 2.5 | 5.4 | 9.5 | 4.1 | 9.2 |
| $M_{F2}$ | 1.3 | 0.6 | 1.3 | 3.5 | 1.5 | 3.4 |
| $\Delta G$ | 0.486 | 0.035 | 0.486 | 0.370 | 0.277 | 0.369 |
| $\Delta Q$ | 15.648 | 0.504 | 4.296 | X[a] | −0.949 | −2.902 |

[a]The result is very large, and it is incredible.

**Table 5.** Calculated Results of Shock Properties Using the Best Fit Solutions

| | Shock 1 | | | Shock 2 | | |
|---|---|---|---|---|---|---|
| | Mth1 | Mth2 | Mth3 | Mth1 | Mth2 | Mth3 |
| $\hat{n}$ | 0.996 | 0.973 | 0.973 | 0.989 | 0.986 | 0.986 |
| | 0.088 | 0.228 | 0.230 | −0.142 | 0.166 | 0.165 |
| | −0.018 | 0.029 | 0.019 | −0.053 | 0.028 | 0.032 |
| y | 2.2 | 2.2 | 2.2 | 1.6 | 1.6 | 1.6 |
| m | 2.1 | 2.1 | 2.1 | 1.6 | 1.6 | 1.6 |
| u | 2.1 | 2.2 | 2.2 | 1.6 | 1.6 | 1.6 |
| z | 1.0 | 1.0 | 1.0 | 1.0 | 1.0 | 1.0 |
| $\theta_{BN}$ | 76.0 | 67.5 | 67.5 | 88.3 | 70.0 | 70.0 |
| $\theta_{BN2}$ | 83.3 | 79.4 | 79.4 | 88.9 | 77.4 | 77.4 |
| $V_A$ | 39.4 | 39.4 | 39.4 | 41.7 | 41.7 | 41.7 |
| $V_{A2}$ | 55.1 | 55.1 | 55.1 | 51.4 | 51.4 | 51.4 |
| $V_{sn}$ | 100.6 | 97.4 | 97.3 | −50.4 | −29.2 | −27.2 |
| $M_A$ | 5.6 | 5.5 | 5.5 | 8.8 | 8.3 | 8.3 |
| $M_{A2}$ | 1.8 | 1.8 | 1.8 | 4.4 | 4.1 | 4.1 |
| $M_{AN}$ | 23.1 | 14.5 | 14.5 | X[a] | 24.3 | 24.3 |
| $M_{AN2}$ | 15.6 | 9.7 | 9.7 | X[a] | 19.0 | 19.0 |
| $M_F$ | 5.5 | 5.4 | 5.4 | 8.6 | 8.1 | 8.1 |
| $M_{F2}$ | 1.2 | 1.2 | 1.2 | 3.6 | 3.5 | 3.5 |
| $\Delta G$ | 0.394 | 0.391 | 0.391 | 0.370 | 0.368 | 0.368 |
| $\Delta Q$ | 1.753 | 0.559 | 0.559 | X[a] | 0.560 | 0.560 |

[a]The result is very large, and it is incredible.

Voyager 2 from behind so that Voyager 2 moves back into the solar wind. The initial crossing which put Voyager 2 into the heliosheath occurred in the data gap. The angle between the shock normal and the upstream magnetic field is around 70°, which confirms the perpendicular shock nature. Due to the uncertainties in measurements of the field in the outer heliosphere and/or interplanetary disturbances, the magnetic field in outer heliosphere is often different form the Parker angle - a 20° deviation from the Parker spiral is not unusual [*Burlaga. et al.*, 2003]. The density ratio for the termination shock is about 2.2, which is also consistent with our model prediction [*Wang and Belcher*, 1999]. For the crossing event during DOY 243.99-244.012(shock 2), the termination shock moves also mainly in the radial direction, but with a speed of about 30 km $s^{-1}$, which indicates that the termination shock moves toward the Sun and puts Voyager 2 into the heliosheath. The angle between the shock normal and the upstream magnetic field is not significantly different from the shock 1 event. The density ratio for the termination shock is about 1.6, which is different from that of shock 1.

## 3. Discussion and Summary

[13] A historical event, Voyager 2 reached the termination shock region and entered the heliosheath at a distance of about 83.6 AU on August 30, 2007. The working Plasma Science instrument make it possible to study the characteristics of the termination shock for the first time. The termination shock moves back and forth, which caused multiple crossings of the termination shock by Voyager 2. Using means directly from observations, different methods to determine the shock normal do not agree very well. However, by using the best fit solution of the Monte-Carlo method first introduced into the shock fitting procedures by *Lin et al.* [2006], we are able to determine a shock's upstream and downstream conditions more accurately, and thus make the calculation of the shock parameters more reliable.

[14] For the two crossing events of the termination shock by Voyager 2 during DOY 243.819-243.875 (shock 1) and DOY 243.99-244.012 (shock 2), the termination shock moved back and forth almost in the radial direction, with the angle between the shock normal and the upstream magnetic field of around 70°, which confirms the perpendicular shock nature. In the case of first crossing, the termination shock moved away from the Sun with a speed of about 100 km $s^{-1}$, whereas the termination shock moved toward Sun with a speed of about 30 km $s^{-1}$ for the second crossing. For both crossing events, the flow is found to be still supersonic with respect to the thermal ions downstream of the termination shock, probably due to the fact that most of the solar wind energy is transferred to the pickup ions. The density ratios of the termination shock are 2.2 and 1.6, respectively. The reason why the density ratio changed so significantly within such a short time period (~1 day) might relate to the pickup processes of interstellar neutrals, which also modify the Rankine-Hugoniot relations by introducing equivalent terms in both momentum flux and energy flux equations (i.e. $\Delta G$ and $\Delta Q$ in Table 4 and 5). The quantitative study of their association needs further investigation and is beyond the scope of this paper.

[15] **Acknowledgments.** We thank J. K. Chao for providing the shock fitting program. This work was supported by grants NNSFC 40621003,40325010 and in part by the Specialized Research Fund for State Key Laboratories of China. J.D. Richardson also received support from NSF grant ATM-0207775.

## References

Abraham-Shrauner, B. (1972), Determination of magneto hydrodynamic shock normals, *J. Geophys. Res.*, *77*, 736.
Burlaga, L. F., N. F. Ness, and J. D. Richardson (2003), Sectors in the distant heliosphere: Voyager 1 and 2 observations from 1999 through 2002 between 57 and 83 AU, *J. Geophys. Res.*, *108*(A10), 8028, doi:10.1029/2003JA009870.
Burlaga, L. F., N. F. Ness, M. H. Acuna, R. P. Lepping, J. E. P. Connerney, and J. D. Richardson (2008), Magnetic fields at the solar wind termination shock, *Nature*, *454*, 75, doi:10.1038/nature07029.
Chao, J. K. (1970), Interplanetary collisionless shock waves, *Rep. CSR TR-70-3*, Cent. for Space Res., Mass. Inst. of Technol., Cambridge.
Colburn, D. S., and C. P. Sonett (1966), Discontinuities in the solar wind, *Space Sci. Rev.*, *5*, 439.
Lin, C. C., J. K. Chao, L. C. Lee, L. H. Lyu, and D. J. Wu (2006), A new shock fitting procedure for the MHD Rankine-Hugoniot relations for the case of small $He^{2+}$ slippage, *J. Geophys. Res.*, *111*, A09104, doi:10.1029/2005JA011449.
Richardson, J. D., J. C. Kasper, C. Wang, J. W. Belcher, and A. J. Lazarus (2008), Voyager 2 plasma observations near the termination shock, *Nature*, *454*(78), doi:10.1038/nature07024.
Stone, E. D., A. C. Cummings, F. B. McDonald, B. C. Herikkila, N. Lai, and W. R. Webber (2008), An asymmetric solar wind termination shock, *Nature*, *454*(71), doi:10.1038/nature07022.
Wang, C., and J. W. Belcher (1999), The heliospheric boundary response to large-scale solar wind fluctuations: A gasdynamic model with pickup ions, *J. Geophys. Res.*, *104*, 549.
Zank, G. P. (1999), Interaction of the solar wind with the local interstellar medium: A theoretical perspective, *Space Sci. Rev.*, *89*, 413.

H. Li and C. Wang, State Key Laboratory of Space Weather, Center for Space Science and Applied Research, Chinese Academy of Sciences, P.O. Box 8701, Beijing 100190, China. (cw@spaceweather.ac.cn)

J. D. Richardson, Kavli Institute for Astrophysics and Space Research, Massachusetts Institute of Technology, 37-655, Cambridge, MA 02139, USA. (jdr@space.mit.edu)